SKB

TECHNICAL REPORT 86-04

Hydrogen production in α-irradiated bentonite

Trygve Eriksen
Royal Institute of Technology, Stockholm, Sweden
Hilbert Christensen
Studsvik Energiteknik AB, Nyköping, Sweden
Erling Bjergbakke
Risø National Laboratory, Roskilde, Denmark

March 1986

SVENSK KÄRNBRÄNSLEHANTERING AB
SWEDISH NUCLEAR FUEL AND WASTE MANAGEMENT CO
BOX 5864 S-102 48 STOCKHOLM
TEL 08-665 28 00 TELEX 13108-SKB

HYDROGEN PRODUCTION IN α-IRRADIATED BENTONITE

Trygve Eriksen
Royal Institute of Technology, Stockholm, Sweden

Hilbert Christensen
Studsvik Energiteknik AB, Nyköping, Sweden

Erling Bjergbakke
Risø National Laboratory, Roskilde, Denmark

March 1986

Hydrogen production in α-irradiated bentonite.

Trygve E Eriksen[1], Hilbert Christensen[2] and Erling Bjergbakke[3]

1) Department of Nuclear Chemistry
The Royal Institute of Technology
S-100 44 Stockholm 70

2) Studsvik Energiteknik AB
S-611 82 Nyköping

3) Risø National Laboratory
DK-4000 Roskilde, Denmark

Abstract

The hydrogen production in α-irradiated (dose rate 73 $rad \cdot s^{-1}$) compacted water-saturated bentonite (ρ = 2.12 $g \cdot cm^{-3}$) has been determined experimentally using a gaschromatographic technique. Hydrogen concentration in the clay pore water and hydrogen diffusion out of the irradiated bentonite have been calculated using a homogeneous reaction model.

The calculated amount of hydrogen diffusing out of the bentonite depends on the Fe^{2+} and HCO_3^- concentration in the pore water.

Agreement between experimental and calculated results can be obtained if it is assumed that a 20 μm layer of water is formed between the clay and the α-source.

CONTENTS

INTRODUCTION

The effect of radiation on water-carrying geologic material (1,2) may be due to direct radiation damage and changes in the redox properties of the water phase.

The primary oxidizing and reducing species formed on radiolysis of water will react with solutes in the ground water and the redox potential is therefore strongly dependent on the water composition, e.g. pH, concentration of carbonate and Fe^{2+}.

The primary radiolytic yields, i.e. G-values of the radicals e^-_{aq}, $H\cdot$, OH and of the molecular products H_2, H_2O_2, O_2 are strongly dependent on the LET (Linear Energy Transfer) of the radiation, the G-values of molecular products increasing with increasing LET at the expense of the yield of radicals.

Due to its high diffusivity and low reactivity H_2 may diffuse away from the irradiated volume. The oxidizing species are more reactive and may thereby possibly create a migrating redox front as proposed by Neretnieks (3,4).

In an earlier experimental study Eriksen and Jacobsson measured the production and diffusion of H_2 away from β^- and γ irradiated volumes of compacted bentonite (5). The experimental results were in fair agreement with the H_2 production calculated by Christensen and Bjergbakke using a homogeneous reaction model (6).

The present report deals with experimental determination and theoretical calculation of H_2 production in α-irradiated compacted water saturated bentonite.

Experimental

Materials: The bentonite used in the present study was the American Colloid Co type Mx-80 granulated Na bentonite. The bentonite was compacted to a density of 1.8 $g \cdot cm^{-3}$ and equilibrated with synthetic ground water solution in a swelling pressure oedometer. The ground water (table 1) was continuously deoxygenated by Ar (AGA-Sr quality) purging during the equilibration.

Irradiation: After water saturation, the oedometer was opened and an Am-241 foil (Amersham) mounted as shown in Fig. 1. This operation was carried out in a glove box with Ar-atmosphere. The oedometer filterstone on the other side of the compacted bentonite was flushed with Ar at differing times after the onset of irradiation, using two gas tight syringes, and the H_2 diffusing through the 8 mm thick bentonite was obtained from gaschromatographic analysis of the flushing gas with an Argograf (Aga).

The radiation source consisted of Am-241 with the decay characteristics $t_{1/2}$ 458 y and E_α 5.486 (86%), 5.443 MeV (12.7%) incorporated in a gold matrix on silver backing and covered on the α-emitting face by a ∿ 2 μm thick gold-palladium alloy. The diameter of the active surface was 25 mm and the nominal activity 900 μCi.

The activity and degraded α-spectrum (due to energy losses in the gold/palladium layer) of the radiation source were measured with a surface-barrier detector as demonstrated in figure 2. The distance between the detector and the Am-241 source was 730 mm and collimators were used to expose the detector to varying fractions of the active surface area. The measurements were carried out at low pressure (< 20 μm Hg) to avoid any additional degradation of the α-spectrum recorded.

The dose rate was obtained by immersing the Am-241 foil in slightly acid water and measuring the H_2 production.

EXPERIMENTAL RESULTS

The α-spectrum of the radiation source is depicted in figure 3 together with an Am-241 reference spectrum. As seen the α-spectrum has a broader energy distribution and the mean α-energy is about 0.9 MeV lower than for the Am-241 reference. The total counting rate of the 4.6 MeV α-peak is plotted vs the fraction (uncovered/total) active source area in figure 4. Treating the partially covered Am-foil as a point source the geometrical factor i.e. the solid angle seen by the detector (figure 2) is given by $\frac{\pi/4\cdot(15.6)^2}{4\pi\cdot(730)^2} = 2.85\cdot10^{-5}$ and from the slope of the plot in figure 4 the activity of the radiation source was calculated to be 966 μCi. The production rate of H_2 in slightly acid water, obtained from the slope of the accumulated H_2 vs irradiation time plot in figure 5, was $8.4\cdot10^{-11}$ mol·min^{-1}.

Assuming 2π-irradiation geometry, the energy deposition rate is $0.5\cdot966\cdot10^{-6}\cdot3.7\cdot10^{10}\cdot4.6\cdot10^{6} = 8.22\cdot10^{13}$ ev·sec^{-1}. The radio-

lytic yield $G(H_2)$ is thus 1.03 molecules·(100 eV)$^{-1}$. Whereas the yields for β^- and γ radiations are well known, this is not the case for α-radiation. Primary G-values published by several authors (7-9) are given in table 1 together with "best estimate values" given by Christensen and Bjergbakke (10). Based on the "best estimate values" the expected G-value for H_2-production in acid solution is $G(H_2)_{tot} = G(H_2) + 1/2[G(H\cdot)+G(e^-_{aq})] = 1.43$ molecules·(100 eV)$^{-1}$, ie ∿40 per cent higher than the G-value calculated from experimental data and assuming 2¶-geometry.

The production rate (dH_2/dt) in compacted water saturated bentonite ($\rho \sim 2.12$ g·cm^{-3}) was found from figure 6 to be $7\cdot10^{-11}$ mol·min^{-1}.

COMPUTER CALCULATIONS

Calculations have been carried out, using a computerized radiation chemical model described earlier (10). The actual reaction mechanism and rate constants used in this work are given in table 3.

Irradiation dose: In calculating the dose rate, the range in water for 4,6 MeV α-particles was taken to be (11) 37 and 17 μm in water and compacted water saturated bentonite (ρ = 2,12 g·cm^{-3}) respectively. Assuming 2Π-geometry the dose rate D_R is then given by

$$D_R = 8{,}22\cdot10^{13}/\Pi\cdot(1.25)^2\cdot37\cdot10^{-4} = 4.53\cdot10^{15} \text{ ev}\cdot\text{g}^{-1} = 73 \text{ rad}\cdot\text{sec}^{-1}$$

Energy transfer bentonite to water is assumed to increase the dose rate with a factor of 1.3 to 94 rad/s.

Irradiated volume: In the initial calculations it was assumed that the radiation was absorbed within the range 17 μm in bentonite containing about 25 % of water. The total volume is then $8.3 \cdot 10^{-3}$ cm^3 and the irradiated water volume was $2.06 \cdot 10^{-3}$ cm^3. In a second phase the possibility of a thin layer of water (without clay particles) close to the α-source was considered. If a 20 μm water layer is assumed the irradiated water volume V will be:

$$V = 20 \cdot 10^{-4} \cdot 4.9 + \frac{(37-20)}{2.19} \cdot 10^{-4} \cdot 0.25 \cdot 4.9 = 1.08\ 10^{-2}\ cm^3$$

Irradiated water: The irradiated water contains Fe^{2+} which is leached continously from the bentonite (5). In the calculation it has been assumed that a constant Fe^{2+} concentration is maintained in the water. The Fe^{2+} is oxidized to Fe^{3+}, which is assumed to precipitate above concentrations of 10^{-6} M. The water is also assumed to contain HCO_3^-/CO_3^{2-}.

At a pH of about 8 the predominant form is HCO_3^-. (The rate constant with OH and HCO_3^- or CO_3^{2-} differ by one order of magnitude.)

A number of calculations with varying composition of the water has been carried out. The compositions are given in table 4.

Diffusion: The diffusivity of hydrogen in the bentonite disc was estimated from the hydrogen break through in figure 6 to be 6.5×10^{-7} cm^2/s. Using Fick' s law:

$$\frac{dn}{dt} = A \cdot D \cdot \frac{dc}{dx}$$

where

$\frac{dn}{dt}$ = Diffusion rate of hydrogen, in $mol \cdot s^{-1}$

A = Area, in dm^2

D = Diffusion coefficient, in $dm^2 \cdot s^{-1}$

$\frac{dc}{dx}$ = Concentration gradient, in $mol \cdot dm^{-3} \cdot dm^{-1}$

$$\frac{dn}{dt} = \frac{4.9 \cdot 10^{-2} \cdot 6.5 \cdot 10^{-7} \cdot 10^{2} \cdot C}{0.8 \cdot 10^{-1}}$$

As $n = C \cdot V$ (V = volume) with
$V = 8.3 \cdot 10^{-3} \cdot 10^{-3}\ dm^3$ we get

$$\frac{dc}{dt} = \frac{4.9 \cdot 6.5 \cdot 10^{-10} \cdot C}{8.3 \cdot 10^{-6} \cdot 0.8} = 4.80 \cdot 10^{-4} \cdot C$$

corresponding to a diffusion rate constant of $4.8 \cdot 10^{-4}\ s^{-1}$.

DISCUSSION

Plot of calculated hydrogen concentration in the pore water and the accumulated amount of hydrogen diffusion out of the irradiated bentonite volume vs time are depicted in figure 7. Steady state conditions are clearly obtained in less than 6 h.

The hydrogen production, being equal to the equilibrium transport, and the hydrogen concentration in pore water for the various conditions are summarized in table 5.

In the case of low LET-irradiation Fe^{2+} and HCO_3^- would be supposed to protect H_2 by scavenging of OH radicals and thus increase the yield, see reactions 80 and 105 in table 3.

As can be seen from Table 6 the opposite seems to be the case for α-irradiation: higher Fe^{2+} concentrations give lower hydrogen yields. The explanation for this is that in the case of α-irradiation the radical yields are low and the molecular yields (H_2 and H_2O_2) are high. H_2O_2 reacts in reactions 9 and 113. This means that in the presence of increasing amounts of Fe^{2+} the concentration of H_2O_2 is decreasing and through reaction 113 an increasing concentration of OH is obtained,

$$-dH_2/dt = k_{12} \cdot [OH] \cdot [H_2] = 4 \cdot 10^7 \cdot [OH] \cdot [H_2]$$

$$-dH_2/dt = k_{124} \cdot [H_2] = 4.8 \cdot 10^{-4} \cdot [H_2]$$

i.e. when

$$OH > \frac{4.8 \cdot 10^{-4}}{4 \cdot 10^7} = 1.2 \cdot 10^{-11} \text{ mol} \cdot \text{dm}^{-3}$$

the main part of the H_2 molecules is decomposed instead of diffusing out of the system.

Calculations based on the initial assumption of a homogenous distribution of clay particles and water in the irradiated compacted water saturated bentonite and 30 percent energy transfer from the solid particles to pore water give lower hydrogen production than obtained experimentally.

The experimental yield of 7×10^{-11} mol·min^{-1} would give a $G(H_2)$ value of 5.8 if all the assumptions were correct. Such a high G-value can hardly be explained on the basis of the present knowledge on α-radiolysis.

A possible explanation for the paradox could be the existence of a thin water layer adjacent to the α-source. If we assume a 20 μm water layer a good agreement between experiment and calculation is obtained, see Table 5.

CONCLUSIONS

Calculations of α-radiolysis of bentonite/water mixtures at a dose rate of 73 rad/s have shown that the amount of hydrogen which diffuses out through a 8 mm thick layer of bentonite depends on the concentrations of Fe^{2+} and carbonate ions present in the water.

Higher concentrations of Fe^{2+} give lower yields of hydrogen. Agreement with experimental results can be obtained if it is assumed that a 20 μm water layer exists closest to the α-source.

ACKNOWLEDGEMENTS

The experimental work by S.O. Engman is gratefully acknowledged.

References

1) V I Spitsyn, B D Balukova and M K Savushkina
"Influence of Irradiation with Gammaquanta and Beam of Accelerated Electrons on the Sorption Parameters of Clay, Minerals of the Montmorrillonite Group" in S.Topp (Ed) Scientific Basis for Nuclear Waste Management Vol 4, p 703 Elsevier, NY (1982).

2) D B Curtis and A J Gancarz
"Radiolysis in nature: Evidence from the Oklo natural reactors". KBS TR 83-10 (1983).

3) I Neretnieks
"The movement of a redox front downstreams from a repository for nuclear waste". KBS TR 82-16 (1982).

4) I Neretnieks and B Åslund
"Two dimensional movements of a redox front downstreams from repository for nuclar waste", KBS TR 83-68 (1983).

5) T E Eriksen and A Jacobsson
"Radiation effects on the chemical environment in a radioactive waste repository". KBS TR 83-27 (1982)

6) H Christensen and E Bjergbakke
"Radiolysis of ground water from HWL stored in copper canisters". KBS TR 82-02 (1982).

7) P Cohen
"Water coolant technology of power reactors."
Gordon and Breach NY 1969.

8) N Bibler
J Phys Chem, 78, 211 (1974)

9) W G Burns, H E Simic
J Chem Soc Faraday Trans I, 77, 2803, (1981).

10) H Christensen and E Bjerkbakke
Radiolysis of ground water from spent fuel.
KBS TR 82-18, (1982) p 16

Table 1

Composition of synthetic ground water.

Species	Conc. mg dm^{-3}
HCO_3^-	123
SO_4^{2-}	9.6
Cl^-	70
SiO_2 (tot)	12
Ca^{2+}	18
Mg^{2+}	4.3
Na^+	65
K^+	3.9

Table 2

Primary G-values for α-radiolysis of water

Reference	G (events/100 eV)							
	$-H_2O$	H_2	H	e^-_{aq}	H_2O_2	HO_2	OH	H^+
Cohen (7)	3.34	1.7	0.16	0.04	1.3	0.3	0.1	0.04
Bibler (8)	2.97	1.28	0.50	0.13	0.98	0.35	0.18	0.13
Burns (9)	2.63	1.17	0.14	0.13	0.92	0.11	0.44	0.13
"Best estimate" Christensen (10)	2.71	1.3	0.21	0.06	0.985	0.22	0.24	0.06

Table 3

Reaction System and Rate Constants

		Rate constant $M^{-1}\ s^{-1}$
RE1:	$OH + OH = H_2O_2$	4 E 9
RE2:	$OH + E^- = OH^- + H_2O$	2 E10
RE3:	$OH + H = H_2O$	2.5 E10
RE6:	$OH + O_2^- = OH^- + O_2$	1 E10
RE9:	$OH + H_2O_2 = H_2O + O_2^- + H^+$	2.25 E 7
RE12:	$OH + H_2 = H_2O + H$	4 E 7
RE19:	$E^- + E^- = 2 \cdot OH^- + H_2$	5 E 9
RE20:	$E^- + H = OH^- + H_2$	2 E10
RE21:	$E^- + HO_2 = HO_2^- + H_2O$	2 E10
RE22:	$E^- + O_2^- = HO_2^- + OH^-$	1.2 E10
RE23:	$E^- + H_2O_2 = OH + OH^- + H_2O$	1.6 E10
RE25:	$E^- + H^+ = H + H_2O$	2.2 E10
RE26:	$E^- + O_2 = O_2^- + H_2O$	2 E10
RE29:	$E^- + H_2O = H + OH^- + H_2O$	2 E 1
RE31:	$H + H = H_2$	1 E10
RE32:	$H + HO_2 = H_2O_2$	2 E10
RE33:	$H + O_2^- = HO_2^-$	2 E10
RE34:	$H + H_2O_2 = OH + H_2O$	6 E 7
RE35:	$H + OH^- = E^-$	2 E 7
RE36:	$H + O_2 = O_2^- + H^+$	2 E10
RE56:	$HO_2 = O_2^- + H^+$	8 E 5
RE57:	$HO_2 + HO_2 = O_2 + H_2O_2$	7.5 E 5
RE58:	$HO_2 + O_2^- = O_2 + HO_2^-$	8.5 E 7
RE61:	$O_2^- + H^+ = HO_2$	5 E10
RE68:	$H_2O_2 + OH^- = HO_2^- + H_2O$	5 E 8

cont

Table 3 cont

		Rate constant $M^{-1}\ s^{-1}$
RE69:	$HO_2^- + H_2O = H_2O_2 + OH^-$	5.735 E 4
RE73:	$H_2O = H^+ + OH^-$	2.599 E-5
RE74:	$H_2O + O_2^{--} = HO_2^- + OH^-$	1
RE76:	$H^+ + OH^- = H_2O$	1.43 E11
RE80:	$OH + CO_3^{--} = CO_3^- + OH^-$	4 E 7
RE82:	$O_2^- + CO_3^- = CO_3^{--} + O_2$	1.5 E 9
RE83:	$H_2O_2 + CO_3^- = CO_3^{--} + O_2^- + 2\cdot H^+$	8 E 5
RE88:	$CO_2 + OH^- = CO_3^{--} + H^+$	1 E 6
RE90:	$H_2O + CO_4^{--} = CO_3^{--} + H_2O_2$	1 E 2
RE91:	$CO_3^- + CO_3^- = CO_4^{--} + CO_2$	6 E 6
RE92:	$CO_3^- + Fe^{++} = CO_3^{--} + Fe^{+++}$	1 E 8
RE105:	$Fe^{++} + OH = Fe^{+++} + OH^-$	3.4 E 8
RE106:	$Fe^{++} + E^- = Fe^{+++} + OH^- + H^-$	1.2 E 8
RE107:	$Fe^{+++} + E^- = Fe^{++} + H_2O$	2 E10
RE108:	$Fe^{++} + H = Fe^{+++} + H^-$	1.3 E 7
RE109:	$Fe^{+++} + H = Fe^{++} + H^+$	1 E 8
RE111:	$Fe^{++} + O_2^- = Fe^{+++} + O_2^{--}$	4 E 8
RE112:	$Fe^{+++} + O_2^- = Fe^{++} + O_2$	4 E 8
RE113:	$Fe^{++} + H_2O_2 = Fe^{+++} + OH + OH^-$	60
RE115:	$H^- + H_2O = H_2 + OH^-$	1
RE116:	$O_2^{--} + H_2O = HO_2^- + OH^-$	1
RE120:	$A = Fe^{++}$	1 E-7
RE121:	$Fe^{++} = A$	45.5
RE122:	$Fe^{+++} + OH^- = FeOH$	1 E 6
RE123:	$FeOH = Fe^{+++} + OH^-$	2 E-9
RE124:	H_2 = DUMMY1	4.8 E-4
RE125:	O_2 = DUMMY2	4.8 E-4

Table 4

Specification of calculation cases

Case No	Concentrations, M Fe^{++}	HCO_3^-/CO_3^{2-}	Σkc
1	2.2E - 7	6.5E - 5	3.3×10^3
2	2.2E - 6	6.5 E - 4	3.3×10^4
3	2.2E - 8	6.5E - 6	3.3×10^2
4	2.2E - 6	2.17E - 5	1.62×10^4
4a	0	4.05E - 5	1.62×10^4
4b	4.76E - 6	0	1.62×10^4

Table 5

Calculated H_2-production and $G(H_2)$-values on α-radiolysis.

Case no	Fe^{2+} conc μM	$dH_2/dt \cdot 10^{11}$(A) mol·min^{-1}	$dH_2/dt \cdot 10^{11}$(B) mol·min^{-1}	$G(H_2)^{(B)}$ molecules·(100eV)$^{-1}$
1	0.22	1.46	7.7	1.21
2	2.2	1.30	6.8	1.08
3	0.02	1.52	8.0	1.26
4	2.2	1.09	5.7	0.90
4a	0	1.54	8.1	1.28
4b	4.8	0.70	3.7	0.58

Experimental yield: $7.0 \cdot 10^{-11}$ mol/min

A: Compacted water saturated bentonite (ρ = 2.12 g·m^{-3})

B: Assuming a 20 μm thick waterlayer between the bentonite and the A-241 source (20 μm H_2O, 8 μm bentonite layers)

Table 6

Final concentrations $mol \cdot dm^{-3}$ of various species in the different cases.

Cases	1	2	3	4	4a	4b
OH	8.8E-13	2.5E-12	2.9E-13	5.2E-12	1.8E-13	1.51E-11
e^-_{aq}	1.1E-16	4.7E-16	6.2E-17	4.8E-16	4.1E-17	2.7E-15
Fe^{2+}	2.2E-7	2.2E-6	2.2E-8	2.2E-6	0	4.76E-6
HCO_3	6.5E-5	6.5E-4	6.5E-6	2.17E-5	4.05E-5	0
H_2O_2	3.1E-3	7.4E-4	5.7E-3	7.5E-4	8.9E-3	1.3E-4
O_2	1.3E-4	2.8E-5	1.2E-4	1.4E-5	4.5E-5	8.9E-8
H_2	2.5E-4	2.2E-4	2.6E-4	1.8E-4	2.6E-4	1.2E-4

Figure Captions

Fig. 1

Schematic of Am-241 irradiation cell and gasflushing system.

\\\\\\ filterstone

—— Am-241

//// bentonite ($\rho \sim 2.1$ g·cm^{-3})

Fig. 2

Schematic of geometry for α-spectroscopy of radiation source [pressure < 20 μm Hg].

Fig. 3

α-spectra of Am-241 radiation source (E = 4.6 MeV) and Am-241 reference (E = 5.488 MeV).

Fig. 4

Counting rate plotted vs ratio of (uncovered/total) area of Am-241 radiation source (geometry is given in fig. 2).

Fig. 5

Hydrogen production in slightly acid water (pH$\approx$5, $HClO_4$).

Fig. 6

Hydrogen production in compacted water saturated bentonite [2.12 g·cm^{-3}].

Fig. 7

Hydrogen concentration in pore water and accumulated amount of hydrogen diffused out of irradiated bentonite. Case 1.

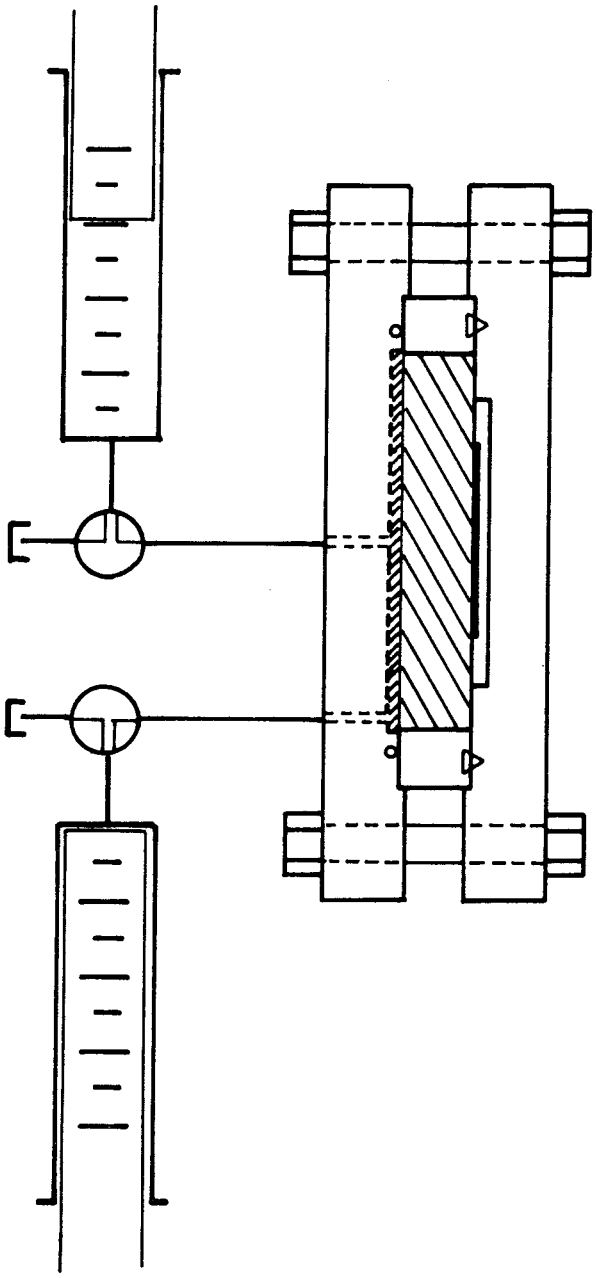

Figure 1

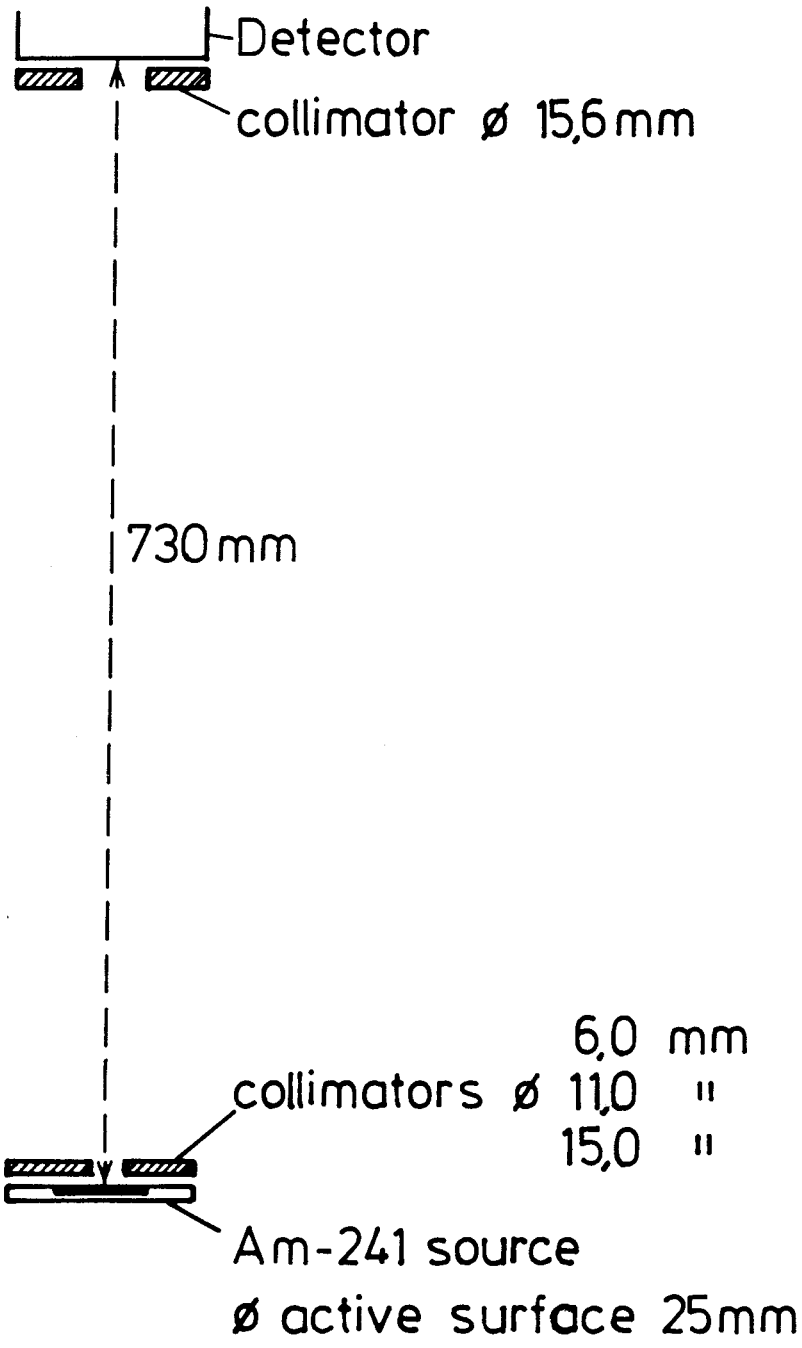
Detector
collimator ø 15,6 mm
730 mm
6,0 mm
collimators ø 11,0 "
15,0 "
Am-241 source
ø active surface 25mm

Figure 2

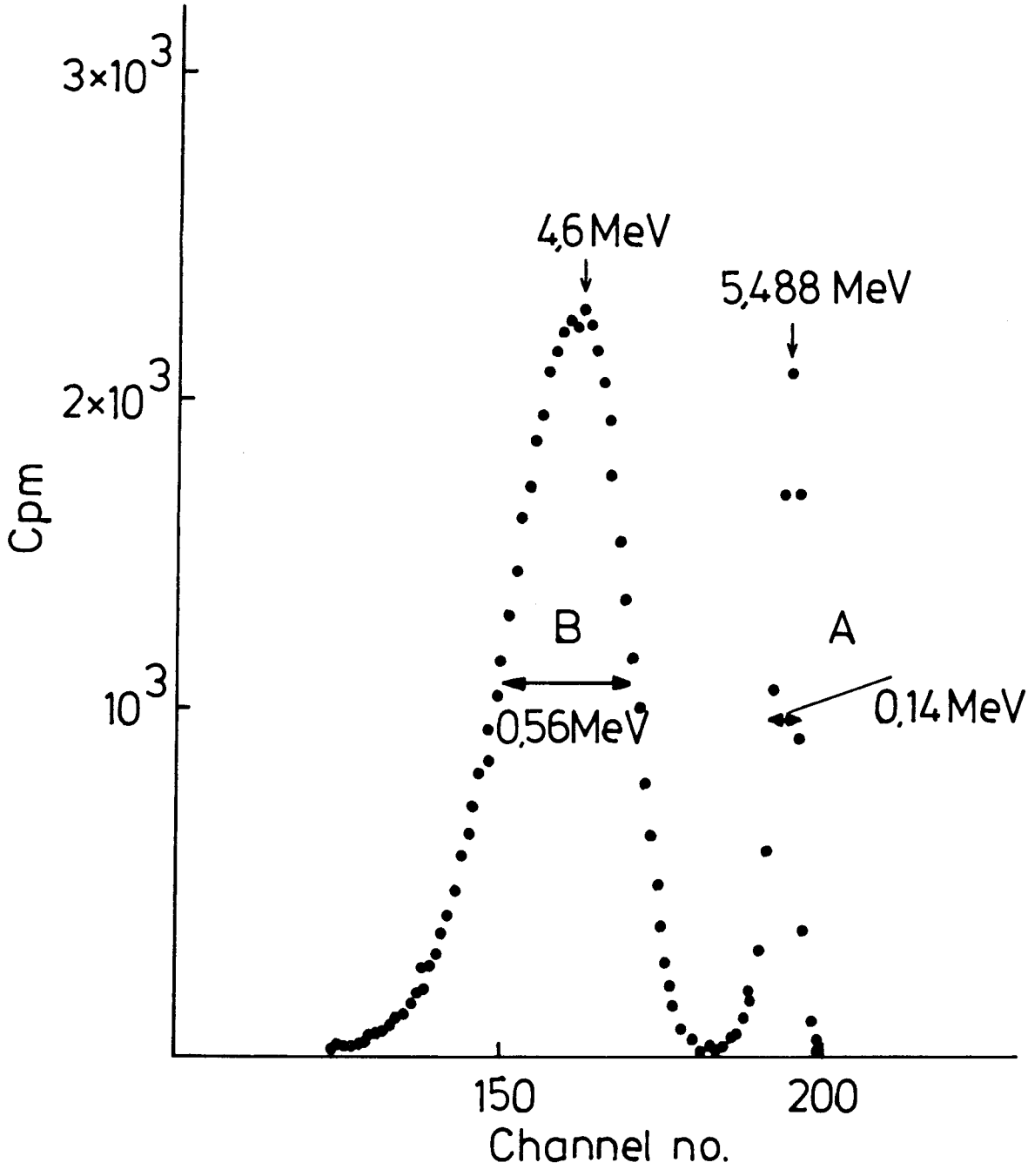
3×10^3
2×10^3
10^3
Cpm
4,6 MeV
5,488 MeV
B
A
0,56MeV
0,14 MeV
150
200
Channel no.

Figure 3

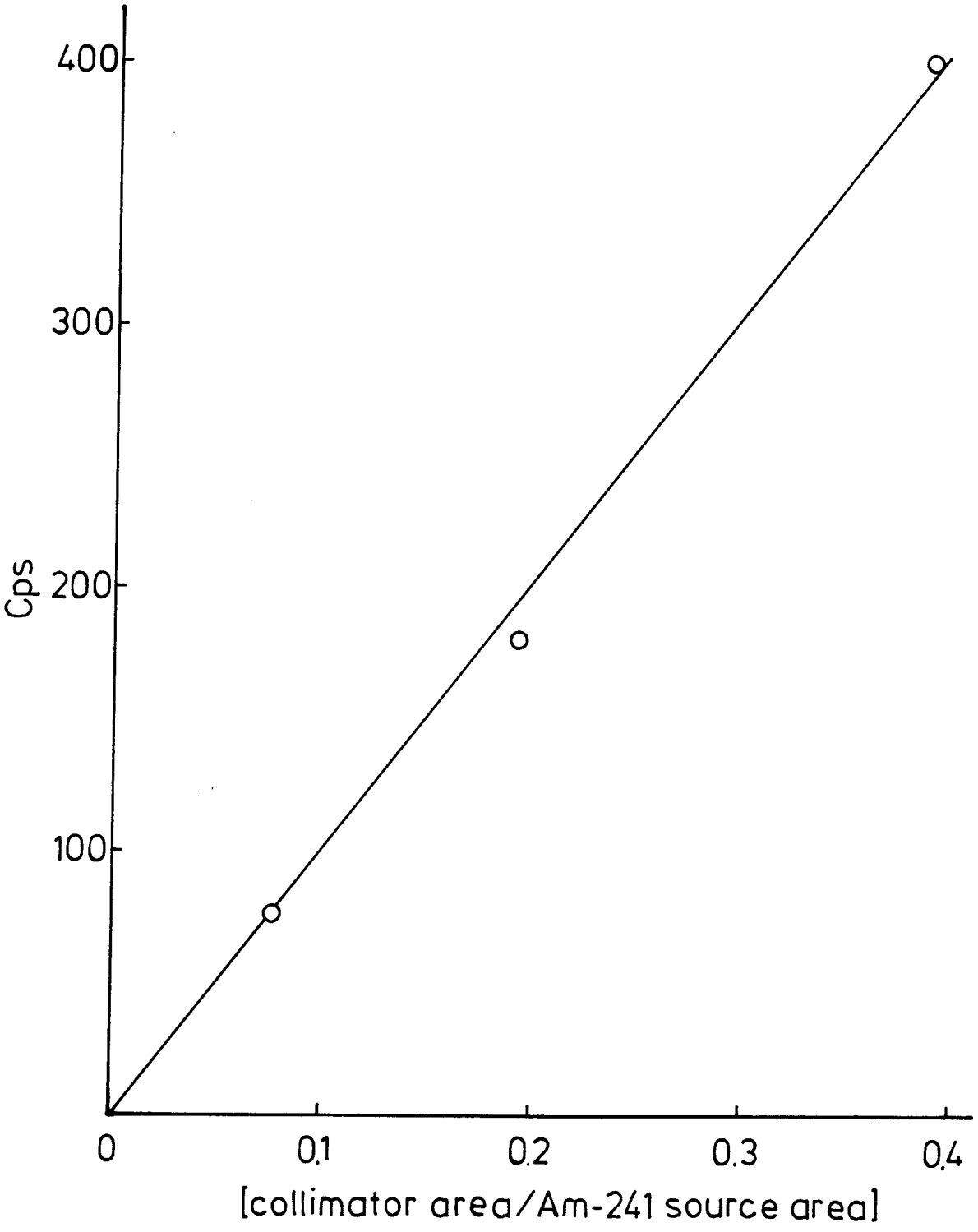
400
300
200
100
Cps
0
0.1
0.2
0.3
0.4
[collimator area/Am-241 source area]

Figure 4

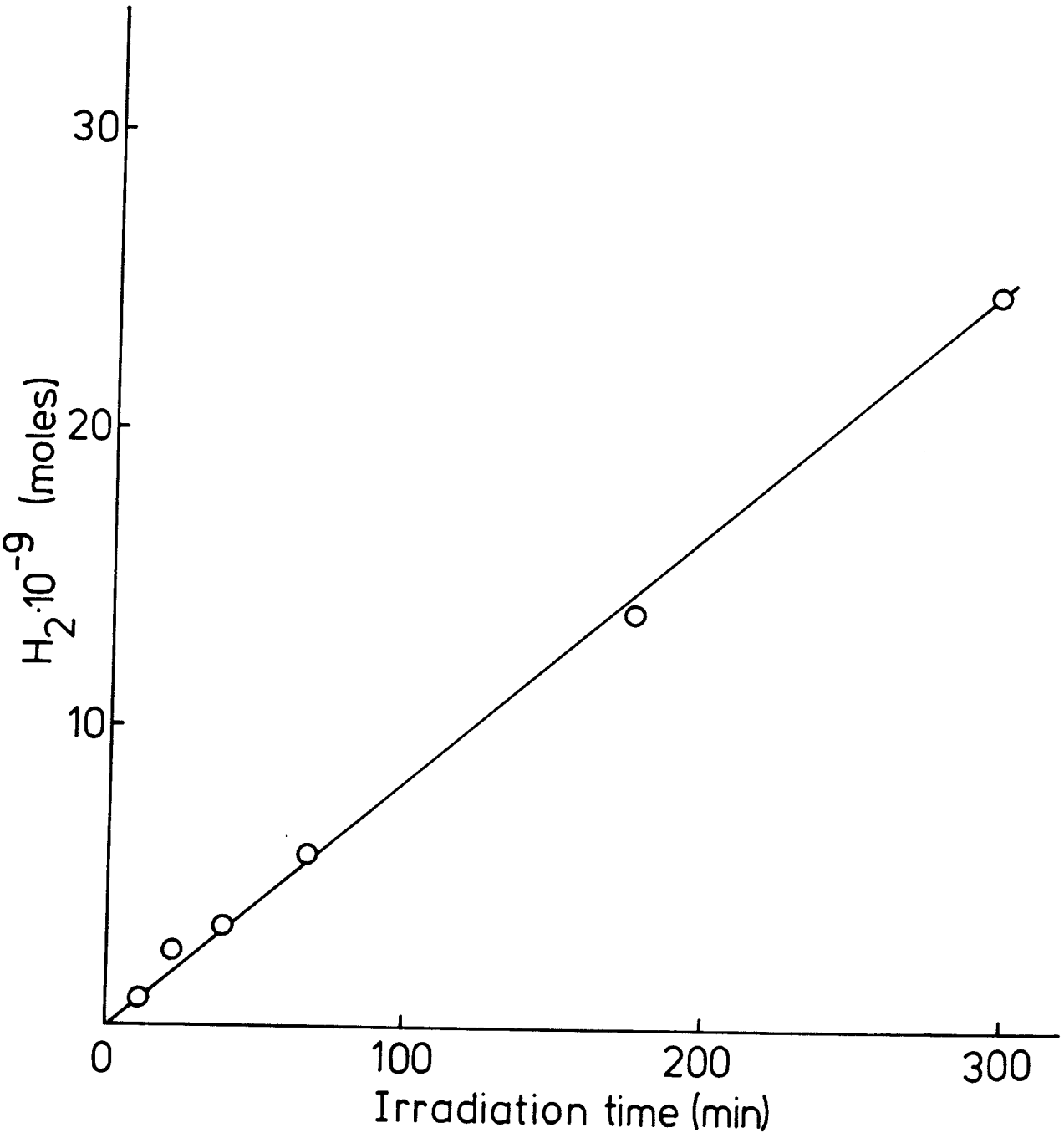

Figure 5

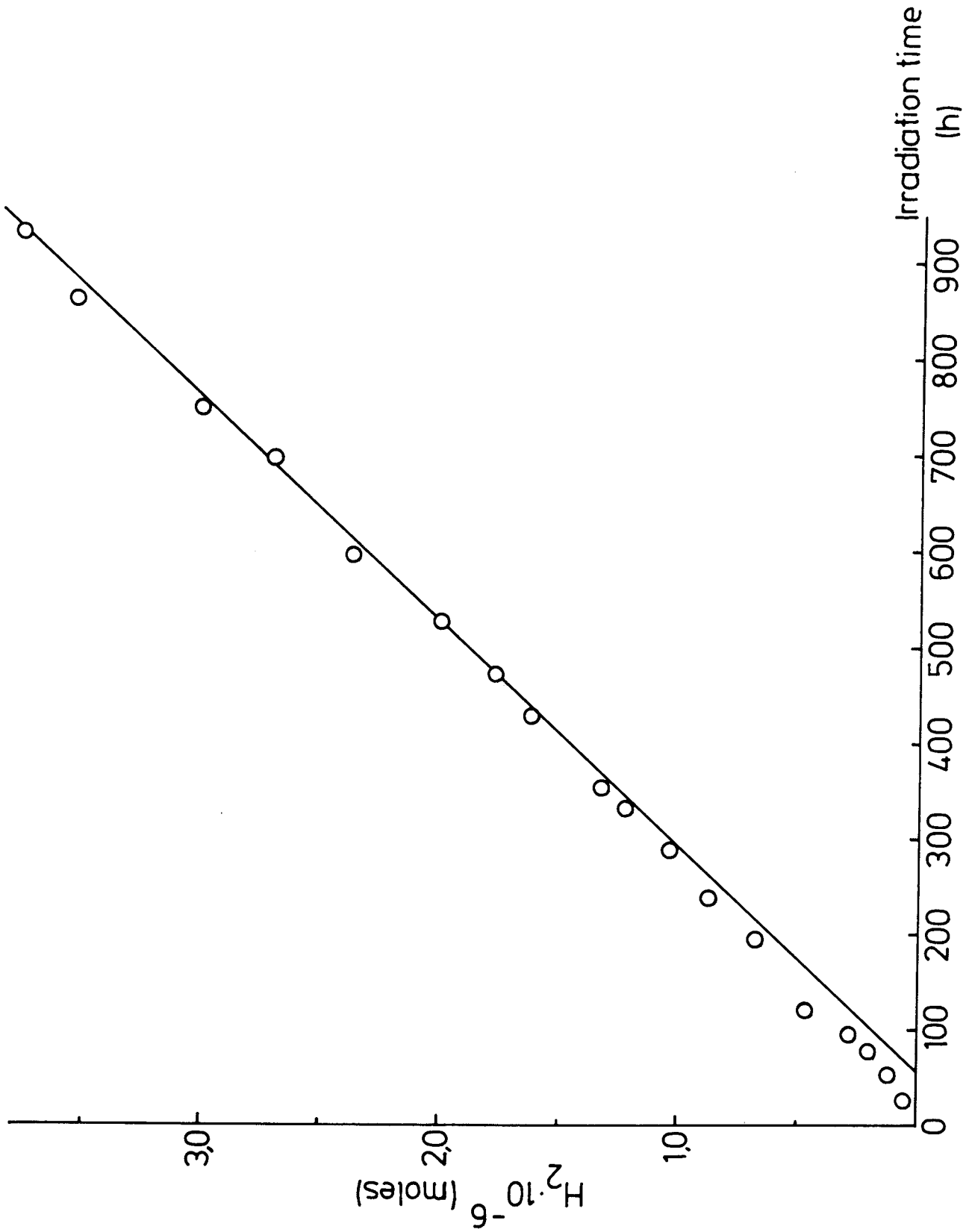
Irradiation time
(h)
0
100
200
300
400
500
600
700
800
900
1,0
2,0
3,0
$H_2 \cdot 10^{-6}$ (moles)

Figure 6

Figure 7

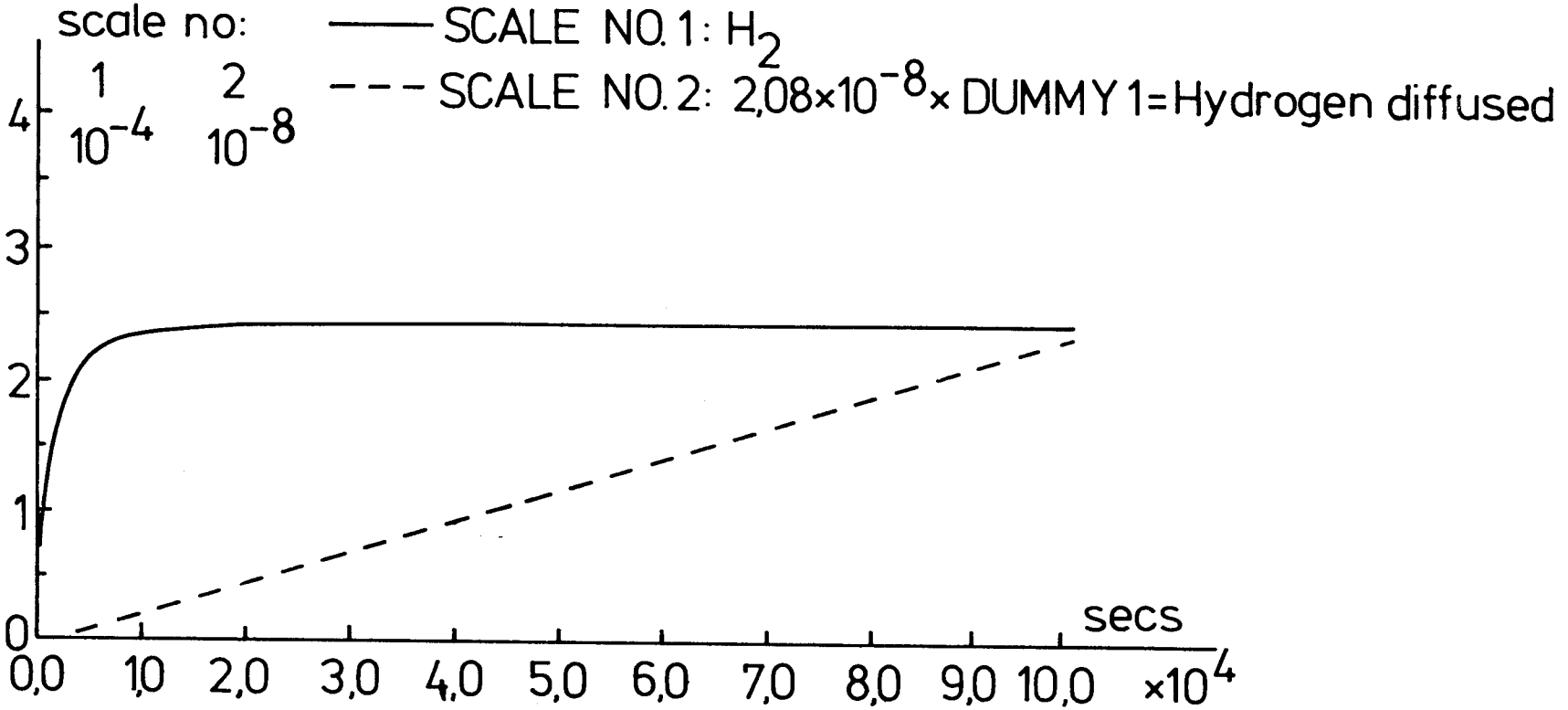
scale no:
1
2
10^{-4}
10^{-8}
SCALE NO. 1: H_2
SCALE NO. 2: $2{,}08\times10^{-8}\times$ DUMMY 1=Hydrogen diffused
4
3
2
1
0
secs
0,0
1,0
2,0
3,0
4,0
5,0
6,0
7,0
8,0
9,0
10,0
$\times10^4$

List of SKB technical reports

1977–78
TR 121
KBS Technical Reports 1 – 120.
Summaries. Stockholm, May 1979.

1979
TR 79–28
The KBS Annual Report 1979.
KBS Technical Reports 79-01 – 79-27.
Summaries. Stockholm, March 1980.

1980
TR 80–26
The KBS Annual Report 1980.
KBS Technical Reports 80-01 – 80-25.
Summaries. Stockholm, March 1981.

1981
TR 81–17
The KBS Annual Report 1981.
KBS Technical Reports 81-01 – 81-16.
Summaries. Stockholm, April 1982.

1982
TR 82–28
The KBS Annual Report 1982.
KBS Technical Reports 82-01 – 82-27.
Summaries. Stockholm, July 1983.

1983
TR 83–77
The KBS Annual Report 1983.
KBS Technical Reports 83-01 – 83-76
Summaries. Stockholm, June 1984.

1984
TR 85–01
Annual Research and Development Report 1984
Including Summaries of Technical Reports Issued during 1984. (Technical Reports 84-01– 84-19)
Stockholm June 1985.

1985
TR 85–01
Annual Research and Development Report 1984
Including Summaries of Technical Reports Issued during 1984.
Stockholm June 1985.

1986
TR 86-01
I: An analogue validation study of natural radionuclide migration in crystalline rock using uranium-series disequilibrium studies
II: A comparison of neutron activation and alpha spectroscopy analyses of thorium in crystalline rocks
J A T Smellie, Swedish Geological Co, A B MacKenzie and R D Scott, Scottish Universities Research Reactor Centre
February 1986

TR 86-02
Formation and transport of americium pseudocolloids in aqueous systems
U Olofsson
Chalmers University of Technology, Gothenburg, Sweden
B Allard
University of Linköping, Sweden
March 26, 1986

TR 86-03
Redox chemistry of deep groundwaters in Sweden
D Kirk Nordstrom
US Geological Survey, Menlo Park, USA
Ignasi Puigdomenech
Royal Institute of Technology, Stockholm, Sweden
April 1, 1986